Inorganica Chimica Acta, *172* (1990) 191–201

Synthesis and Structure Determination of Two Unusual Dirhodium Complexes Having Thiolato and Carbonyl Bridging Ligands

HERBERT SCHUMANN*, STANISLAW JURGIS
Institut für Anorganische und Analytische Chemie, Technische Universität Berlin, D-1000 Berlin 12 (F.R.G.)
MORIS EISEN and JOCHANAN BLUM*
Department of Organic Chemistry, The Hebrew University, Jerusalem 91904 (Israel)

Received July 20, 1989; revised December 13, 1989)

Abstract

Two unusual carbonyl bridged dirhodium complexes $[(CH_3)_2PC_6H_5](CO)Rh(\mu\text{-}CO)(\mu\text{-}SC_6H_{11})_2RhCl_2[(CH_3)_2PC_6H_5]$ (7) and $[(CH_3)_2PC_6H_5]_2ClRh(\mu\text{-}CO)(\mu\text{-}Cl)(\mu\text{-}SC_6H_{11})RhCl[(CH_3)_2PC_6H_5]$ (8) were obtained from the reaction of $[Rh(CO)_2]_2(\mu\text{-}Cl)_2$ (1) with $(CH_3)_2PC_6H_5$ (4) and $(CH_3)_3SiSC_6H_{11}$ (5). Their geometric structures as well as the structure of *trans*-$RhCl(CO)[(CH_3)_2PC_6H_5]_2$ (6) were determined by X-ray diffraction analysis, and qualitative molecular orbital pictures were obtained from extended Hückel molecular orbital (EHMO) calculations. Both dirhodium complexes can be described in terms of the combination of one square pyramid and one octahedron. Complex 6 is square planar and belongs to space group $P\bar{1}$ with $a = 10.277(2)$, $b = 15.881(3)$, $c = 6.025(1)$ Å; $\alpha = 96.60(4)$, $\beta = 93.65(5)$, $\gamma = 83.81(5)^\circ$; $Z = 2$; $R = 0.043$ and $R_w = 0.069$ for 2702 reflections with $I \geqslant 3\sigma_I$. Compound 7 belongs to space group $P2_1/n$ with $a = 11.976(3)$, $b = 22.721(4)$, $c = 14.153(3)$ Å; $\beta = 97.03(5)^\circ$; $Z = 4$; $R = 0.066$ and $R_w = 0.087$ for 3204 reflections with $I \geqslant 3\sigma_I$. The two rhodium atoms are connected by two cyclohexylthiolato bridges and by one carbonyl bridge. The Rh(1)–Rh(2) distance is 2.848 Å, yet EHMO calculations indicate no direct interactions between the two metal atoms. Complex 8 belongs to space group $P2_1/c$ with $a = 15.832(4)$, $b = 11.080$, $c = 21.407(5)$ Å; $\beta = 108.66(5)^\circ$; $Z = 4$; $R = 0.047$ and $R_w = 0.067$ for 3699 reflections with $I \geqslant 2\sigma_I$. Chlorine, carbonyl and cyclohexylthiolato groups serve as bridging ligands. The Rh(1)–Rh(2) distance is of the same order of magnitude as in 7 (2.873 Å), yet the calculations reveal some metal–metal interactions that involve the d(xy) and d(z^2) orbitals of both rhodium atoms. The existence of Rh(1)–Rh(2) interactions is also confirmed by the temperature dependent ESR spectrum.

Introduction

In previous studies [1, 2] we have shown that the reaction of $[Rh(CO)_2]_2(\mu\text{-}Cl)_2$ (1) and tri-tert-butylphosphine, followed by treatment with alkylthiolato- or (arylthiolato)trimethylsilane, gives dirhodium compounds of formula *cis*-$[R_3P(CO)Rh]_2(\mu\text{-}Cl)(\mu\text{-}SR)$ (2), where R = $(CH_3)_3C$. These complexes proved to act as efficient homogeneous catalysts in various hydrogen transfer, carbonylation and rearrangement processes, with retention of both the chlorine and sulfur bridges during the catalyses. The catalytic activities of these dirhodium complexes were found to increase even further by their attachment to various organic and inorganic insoluble supports [3, 4]. Substitution of the tri-tert-butylphosphine reagent by the corresponding arsine, led to analogous catalysts of formula *cis*-$[((CH_3)_3C)_3As(CO)Rh]_2(\mu\text{-}Cl)(\mu\text{-}SR)$ (3) [5]. The application of some phenylated phosphines instead of the bulky $[(CH_3)_3C]_3P$, gave however, mixtures of rhodium complexes that proved difficult to separate [6].

We now wish to report the formation of two carbonyl-bridged dirhodium complexes upon reacting 1 with dimethylphenylphosphine (4) and (cyclohexylthio)trimethylsilane (5), and to present the elucidation of their geometric and electronic structures by X-ray diffraction analysis and by extended Hückel molecular orbital (EHMO) calculations.

Experimental

Reaction of 1 with Dimethylphenylphosphine and 5

A mixture of 100 mg (0.26 mmol) of freshly sublimed (dicarbonylchloro)rhodium dimer (1) (Strem Chemicals) and 73.5 mg (0.52 mmol) of $(CH_3)_2PC_6H_5$ (4) (Strem Chemicals) in 10 ml of degassed toluene was stirred under argon at room temperature for 5 h during which evolution of CO was noticed. To the clear orange solution was syringed dropwise a solution of 48 mg (0.26 mmol)

---

*Authors to whom correspondence should be addressed.

0020-1693/90/$3.50

of $(CH_3)_3SiSC_6H_{11}$ (**5**) [7] in 100 ml of degassed pentane. After 2 h, the brown solid was filtered, washed with pentane, dissolved in 5 ml of a 1:1 mixture of cold MeOH–THF and chromatographed in the cold on silica gel under exclusion of air, using the same mixture of solvents as eluent. The main fraction was subjected to fractional crystallization from MeOH–THF mixtures at −30 °C to give first yellow *trans*-$RhCl(CO)[(CH_3)_2PC_6H_5]_2$ (**6**) [8], and then a mixture of dark red and orange crystals of $[(CH_3)_2PC_6H_5](CO)Rh(\mu\text{-}CO)(\mu\text{-}SC_6H_{11})_2RhCl_2\text{-}[(CH_3)_2PC_6H_5]$ (**7**) and $[(CH_3)_2PC_6H_5)_2ClRh(\mu\text{-}CO)(\mu\text{-}Cl)(\mu\text{-}SC_6H_{11})RhCl[(CH_3)_2PC_6H_5]$ (**8**), respectively, that could, however, be hand separated.

Upon concentration of the mother liquors solid material was obtained that proved difficult to separate, and that is assumed by virtue of the IR and ^{31}P NMR spectra [1, 2], to contain among others, *cis*- and *trans*-$\{((CH_3)_2PC_6H_5)(CO)Rh]_2(\mu\text{-}Cl)(\mu\text{-}SC_6H_{11})$ (**9** and **10**, respectively).

*X-ray Crystallographic Analysis of **6**, **7** and **8***

Data were measured on a PW1100/20 Philips four-circle computer-controlled diffractometer, using Mo Kα ($\lambda = 0.71069$ Å) radiation with a graphite crystal monochromator in the incident beam. The unit cell dimensions were obtained by a least-squares fit of 18 centered reflections in the range of $11 \leqslant \theta \leqslant 14°$ for **6** and of 24 centered reflections in the range of $10 \leqslant \theta \leqslant 14°$ for **7** and **8**. Intensity data were collected using the ω–2θ technique to a maximum 2θ of 45° (**7** and **8**) or 50° (**6**). The scan width, $\Delta\omega$, for each reflection was $1.00 + 0.35 \tan\theta$ with a scan speed of $0.05° \text{ min}^{-1}$. Background measurements were made for a total of 20 s at both limits of each scan. Three standard reflections were monitored every 60 min. No systematic variations in intensities were found. Intensities were corrected for Lorentz and polarization effects. All non-hydrogen atoms were found by using the results of the SHELXS-86 [9] direct method analysis [10]. Refinement proceeded to convergence by minimizing the function $\Sigma w(|F_o| - |F_c|)^2$. Final difference peaks less than 0.6 for **6** or 0.8 e/Å^3 for **7** and **8** scattered about the unit cell without a significant feature.

The discrepancy indices $R = \Sigma||F_o| - |F_c||/\Sigma|F_o|$ and $R_w = [\Sigma w(|F_o| - |F_c|)^2/\Sigma(|F_o|)^2]^{1/2}$ are presented with other pertinent crystallographic data in Table 1. Final positional parameters and their standard deviations for all non-hydrogen atoms are given in Tables 2, 3 and 4. Selected bond lengths and bond angles are given in Tables 5, 6 and 7. ORTEP drawings indicating the atom numbering scheme of compounds **6**, **7** and **8** are shown in Figs. 1, 2 and 3, respectively; stereoscopic views of **7** and **8** in Figs. 4 and 5.

Results and Discussion

While both tri-tert-butylphosphine [1, 2] and triphenylphosphine [6] (as well as some alkyldiphenylphosphines [11]) react with $[Rh(CO)_2]_2(\mu\text{-}Cl)_2$ (**1**) and (alkylthio)trimethylsilane to give dirhodium complexes with one bridging chloro and one bridging thiolato group (eqn. (1)), the application of dimethylphenylphosphine (**4**) was found to yield mainly *trans*-carbonylchlorobis(dimethylphenylphosphine)rhodium (**6**) (that was reported to result among other products from **1** and excessive **5** [12]) and two

TABLE 1. Crystallographic data for compounds **6**, **7** and **8**

Compound	**6**	**7**	**8**
Formula	$C_{17}H_{22}ClOP_2Rh$	$C_{30}H_{44}Cl_2O_2P_2Rh_2S_2$	$C_{31}H_{44}Cl_3OP_3Rh_2S$
Formula weight (g mol^{-1})	442.7	839.5	869.8
Space group	$P\bar{1}$	$P2_1/n$	$P2_1/c$
a (Å)	10.227(2)	11.976(3)	15.832(4)
b (Å)	15.8813	22.721(4)	11.080(2)
c (Å)	6.025(1)	14.153(3)	21.407(5)
α (°)	96.60(4)		
β (°)	93.65(5)	97.03(5)	108.66(5)
γ (°)	83.81(5)		
V (Å^3)	969.8(7)	3822.2(9)	3557.8(9)
Z	2	4	4
ρ_{calc} (g cm^{-3})	1.52	1.46	1.62
μ(Mo Kα) (cm^{-1})	10.70	11.08	12.47
No. unique data	3356	4874	4550
No. observed data	2702 ($I \geqslant 3\sigma_I$)	3204 ($I \geqslant 3\sigma_I$)	3699 ($I \geqslant 2\sigma_I$)
R	0.043	0.066	0.047
R_w	0.069	0.087	0.067
w	$(\sigma_F^2 + 0.001563F^2)^{-1}$	σ_F^{-2}	$(\sigma_F^2 + 0.000233F^2)^{-1}$

TABLE 2. Positional parameters and e.s.d.s for **6**

Atom	*x*	*y*	*z*
Rh	0.81770(4)	0.23463(3)	0.54389(8)
Cl	1.0222(2)	0.1527(1)	0.5705(4)
P(1)	0.9092(2)	0.3381(1)	0.7867(3)
P(2)	0.7423(2)	0.1206(1)	0.3141(3)
O	0.5631(5)	0.3392(4)	0.507(1)
C(1)	0.6624(7)	0.2982(4)	0.522(1)
C(2)	0.8031(6)	0.4336(4)	0.880(1)
C(3)	0.7399(7)	0.4372(5)	1.082(1)
C(4)	0.6543(8)	0.5075(6)	1.151(2)
C(5)	0.6316(9)	0.5755(6)	1.024(2)
C(6)	0.694(1)	0.5730(6)	0.826(2)
C(7)	0.7797(8)	0.5000(5)	0.752(1)
C(8)	0.9860(8)	0.2998(8)	1.042(1)
C(9)	1.0455(8)	0.3792(5)	0.669(1)
C(10)	0.5819(6)	0.1376(4)	0.171(1)
C(11)	0.4692(7)	0.1176(7)	0.264(1)
C(12)	0.3467(8)	0.13h1(6)	0.152(2)
C(13)	0.3353(8)	0.1716(5)	−0.047(2)
C(14)	0.4490(8)	0.1919(5)	−0.137(1)
C(15)	0.5700(8)	0.1774(5)	−0.027(1)
C(16)	0.8487(7)	0.0743(5)	0.091(1)
C(17)	0.7312(8)	0.0305(4)	0.470(1)

dirhodium complexes $[(CH_3)_2PC_6H_5](CO)Rh(\mu\text{-}CO)(\mu\text{-}SR)_2RhCl_2[(CH_3)_2PC_6H_5]$ (**7**) and $[(CH_3)_2PC_6H_5]_2ClRh(\mu\text{-}CO)(\mu\text{-}Cl)(\mu\text{-}SR)RhCl[(CH_3)_2PC_6H_5]$ (**8**) (eqn. (2)).

$$(CO)_2Rh(\mu\text{-}Cl)_2Rh(CO)_2 + Me_3SiSR' + PR_3 \xrightarrow{-Me_3SiCl} (R_3P)(CO)Rh(\mu\text{-}Cl)(\mu\text{-}SR')Rh(CO)(PR_3) \qquad (1)$$

$R = (CH_3)_3C$, Ph; $R' = C_6H_{11}$

$$\underset{\mathbf{1}}{(CO)_2Rh(\mu\text{-}Cl)_2Rh(CO)_2} + \underset{\mathbf{4}}{Me_2PhP} + \underset{\mathbf{5}}{Me_3SiSR}$$

$$\xrightarrow{-Me_3SiCl} \underset{\mathbf{6}}{Rh(CO)(Cl)(Me_2PhP)_2}$$

$$+ \underset{\mathbf{7}}{(Me_2PhP)(CO)Rh(\mu\text{-}CO)(\mu\text{-}SR)_2RhCl_2(Me_2PhP)}$$

$$+ \underset{\mathbf{8}}{(Me_2PhP)_2ClRh(\mu\text{-}CO)(\mu\text{-}Cl)(\mu\text{-}SR)RhCl(Me_2PhP)} \qquad (2)$$

$R = C_6H_{11}$

TABLE 3. Positional parameters and e.s.d.s for 7

Atom	*x*	*y*	*z*
Rh(1)	0.5058(1)	0.17964(6)	0.6936(1)
Rh(2)	0.7296(1)	0.19673(5)	0.65026(9)
Cl(1)	0.8545(4)	0.1148(2)	0.6673(3)
Cl(2)	0.8774(4)	0.2642(2)	0.7142(3)
S(1)	0.6636(4)	0.1912(2)	0.8105(3)
S(2)	0.5823(3)	0.2662(2)	0.6301(3)
P(1)	0.3523(3)	0.1856(2)	0.5787(3)
P(2)	0.7844(4)	0.2101(2)	0.5019(3)
O(1)	0.590(1)	0.0984(5)	0.559(1)
O(2)	0.418(1)	0.0666(6)	0.762(1)
C(1)	0.611(1)	0.1396(7)	0.607(1)
C(2)	0.450(1)	0.1084(8)	0.740(1)
C(3)	0.273(1)	0.1167(7)	0.561(1)
C(4)	0.311(1)	0.0725(8)	0.508(1)
C(5)	0.254(1)	0.0196(8)	0.494(1)
C(6)	0.153(2)	0.0114(8)	0.535(1)
C(7)	0.113(2)	0.0571(9)	0.589(1)
C(8)	0.173(1)	0.1100(7)	0.602(1)
C(9)	0.384(1)	0.2055(8)	0.458(1)
C(10)	0.253(1)	0.243(7)	0.608(2)
C(11)	0.741(1)	0.2773(7)	0.444(1)
C(12)	0.803(2)	0.3267(9)	0.470(1)
C(13)	0.764(2)	0.382(1)	0.426(2)
C(14)	0.663(2)	0.384(1)	0.357(1)
C(15)	0.607(2)	0.333(1)	0.332(2)
C(16)	0.645(2)	0.2793(9)	0.378(1)
C(17)	0.942(1)	0.208(1)	0.504(2)
C(18)	0.736(1)	0.1531(8)	0.413(1)
C(19)	0.703(1)	0.1190(7)	0.867(1)
C(20)	0.626(2)	0.1046(9)	0.942(1)
C(21)	0.670(2)	0.044(1)	0.993(2)
C(22)	0.796(2)	0.051(1)	1.040(2)
C(23)	0.871(2)	0.069(1)	0.963(2)
C(24)	0.830(2)	0.1260(8)	0.914(1)
C(25)	0.609(1)	0.3249(7)	0.718(1)
C(26)	0.493(1)	0.3467(8)	0.745(1)
C(27)	0.513(2)	0.4013(8)	0.814(1)
C(28)	0.568(2)	0.4515(7)	0.763(2)
C(29)	0.681(1)	0.4297(7)	0.737(1)
C(30)	0.666(1)	0.3762(7)	0.668(1)

The structure of **6**, of which the spectroscopic data proved to be in full agreement with those previously reported [13], and the structures of the latter dirhodium complexes where $R = C_6H_{11}$ (**7** and **8**, respectively) were determined by X-ray diffraction analysis.

The ORTEP plot (Fig. 1) of *trans*-$Rh(Cl)(CO)[(CH_3)_2PC_6H_5]_2$ (**6**) shows the expected arrangement around rhodium which is in accordance with the structures of other known compounds of the Vaska-complex type [14]. In the crystalline state the phenyl groups of both dimethyl(phenyl)phosphine ligands are at the same side of the molecule orientated towards the carbonyl group. This can be rationalized by an interaction between the electronic systems of the carbonyl group and the aromatic rings, and is in agreement with our EHMO calculations: the overlap population between C(1), C(2), C(10) and O(18) in the same MO is C(1) = 0.21 p (y) + 0.17 p

TABLE 4. Positional parameters and e.s.d.s for 8

Atom	*x*	*y*	*z*
Rh(1)	0.78000(4)	0.25556(6)	0.59255(3)
Rh(2)	0.71573(4)	0.23755(6)	0.70344(3)
Cl(1)	0.7301(1)	0.4298(2)	0.6464(1)
Cl(2)	0.7105(2)	0.3516(2)	0.4850(1)
Cl(3)	0.7766(2)	0.3352(2)	0.8055(1)
S	0.6427(1)	0.1642(2)	0.5984(1)
P(1)	0.8048(2)	0.1013(2)	0.5314(1)
P(2)	0.9158(2)	0.3535(2)	0.6132(1)
P(3)	0.6940(2)	0.703(2)	0.7537(1)
O	0.8821(4)	0.1194(5)	0.7153(3)
C(1)	0.8213(6)	0.1774(8)	0.6824(4)
C(2)	0.8568(6)	−0.0335(7)	0.5756(4)
C(3)	0.9462(6)	−0.0534(8)	0.5918(5)
C(4)	0.9873(7)	−0.154(1)	0.6273(5)
C(5)	0.9326(8)	−0.2413(9)	0.6457(5)
C(6)	0.8385(8)	−0.2244(9)	0.6279(5)
C(7)	0.8018(6)	−0.1183(8)	0.5926(5)
C(8)	0.7004(6)	0.0457(9)	0.4714(5)
C(9)	0.8724(7)	0.1386(9)	0.4786(5)
C(10)	1.0198(6)	0.2750(8)	0.6182(5)
C(11)	1.0629(7)	0.2955(9)	0.5698(5)
C(12)	1.1456(8)	0.238(1)	0.5792(6)
C(13)	1.1840(7)	0.168(1)	0.6327(7)
C(14)	1.1413(7)	0.143(1)	0.6802(6)
C(15)	1.0587(6)	0.1985(9)	0.6717(5)
C(16)	0.9503(6)	0.4269(9)	0.6940(5)
C(17)	0.9090(6)	0.4796(8)	0.5563(5)
C(18)	0.5835(6)	0.0746(9)	0.7636(5)
C(19)	0.5149(8)	0.002(1)	0.7254(6)
C(20)	0.4287(9)	0.015(1)	0.7343(9)
C(21)	0.4171(9)	0.092(1)	0.7818(8)
C(22)	0.4851(9)	0.163(1)	0.8175(7)
C(23)	0.5718(6)	0.156(1)	0.8100(5)
C(24)	0.6990(8)	−0.0720(8)	0.7128(6)
C(25)	0.7740(7)	0.043(1)	0.8357(5)
C(26)	0.5487(5)	0.2709(8)	0.5628(4)
C(27)	0.4979(7)	0.283(1)	0.6130(5)
C(28)	0.4167(7)	0.370(1)	0.5812(5)
C(29)	0.3581(6)	0.3244(9)	0.5143(5)
C(30)	0.4116(6)	0.313(1)	0.4668(5)
C(31)	0.4927(6)	0.2222(9)	0.4972(5)

TABLE 5. Selected bond lengths (Å) and angles (°) for 6 with e.s.d.s in parentheses

Bond lengths		Bond angles	
Rh–Cl	2.357(2)	Cl–Rh–P(1)	66.89(7)
Rh–P(1)	2.308(2)	Cl–Rh–P(2)	87.66(7)
Rh–P(2)	2.320(2)	Cl–Rh–C(1)	179.3(2)
Rh–C(1)	1.800(6)	P(1)–Rh–P(2)	174.11(6)
C(1)–O	1.154(8)	P(1)–Rh–C(1)	92.8(2)
P(1)–C(2)	1.825(6)	P(2)–Rh–C(1)	92.7(2)
		Rh–C(1)–O	179.4(6)

TABLE 6. Selected bond lengths (Å) and angles (°) for 7 with e.s.d.s in parentheses

Bond lengths			
Rh(1)–Rh(2)	2.848(2)	Rh(2)–Cl(1)	2.381(4)
Rh(1)–S(1)	2.370(4)	Rh(2)–Cl(2)	2.431(4)
Rh(1)–S(2)	2.390(4)	Rh(2)–S(1)	2.494(5)
Rh(1)–P(1)	2.304(4)	Rh(2)–S(2)	2.356(4)
Rh(1)–C(1)	2.07(2)	Rh(2)–P(2)	2.296(5)
Rh(1)–C(2)	1.90(2)	Rh(2)–C(1)	1.97(2)
Bond angles			
Rh(2)–Rh(1)–S(1)	56.2(1)	Cl(1)–Rh(2)–P(2)	87.1(2)
Rh(2)–Rh(1)–S(2)	52.6(1)	Cl(2)–Rh(2)–C(1)	86.4(5)
Rh(2)–Rh(1)–P(1)	122.1(1)	Cl(2)–Rh(2)–S(1)	89.4(2)
Rh(2)–Rh(1)–C(1)	43.8(5)	Cl(2)–Rh(2)–S(2)	97.1(1)
Rh(2)–Rh(1)–C(2)	124.7(5)	Cl(2)–Rh(2)–P(2)	88.9(2)
S(1)–Rh(1)–S(2)	82.0(1)	Cl(2)–Rh(2)–C(1)	176.3(6)
S(1)–Rh(1)–P(1)	170.3(2)	S(1)–Rh(2)–S(2)	80.1(1)
S(1)–Rh(1)–C(1)	88.5(5)	S(1)–Rh(2)–P(2)	175.0(2)
S(1)–Rh(1)–C(2)	97.8(6)	S(1)–Rh(2)–C(1)	87.4(5)
S(2)–Rh(1)–P(1)	89.8(2)	S(2)–Rh(2)–P(2)	95.4(2)
S(2)–Rh(1)–C(1)	81.4(5)	S(2)–Rh(2)–C(1)	84.3(5)
S(2)–Rh(1)–C(2)	176.8(5)	P(2)–Rh(2)–C(1)	94.5(5)
P(1)–Rh(1)–C(1)	95.5(5)	Rh(1)–S(1)–Rh(2)	71.6(1)
P(1)–Rh(1)–C(2)	90.7(6)	Rh(1)–S(2)–Rh(2)	73.7(1)
C(1)–Rh(1)–C(2)	95.4(7)	Rh(1)–C(1)–Rh(2)	89.6(7)
Cl(1)–Rh(2)–Cl(2)	92.1(2)	Rh(1)–C(1)–O(1)	126(1)
Cl(1)–Rh(2)–S(1)	97.7(2)	Rh(2)–C(1)–O(1)	144(1)
Cl(1)–Rh(2)–S(2)	170.6(2)	Rh(1)–C(2)–O(2)	177(2)

(*z*), C(2) = −0.11 p (*x*), C(10) = 0.15 p (*x*) and O(18) = 0.51 p (*y*) + 0.42 p (*z*).

The drawing shown in Fig. 2 and the data listed in Table 6 reveal that the bis-thiolato complex 7 consists of two rhodium atoms with different inner coordination spheres. While Rh(1) is located within a distorted square pyramid with the bridging carbonyl in the apical position, Rh(2) is in a distorted octahedral sphere. Both metal atoms are triply linked by two thiolate groups and one carbonyl group. The existence of an additional bond between the two metal atoms had to be considered, since, on the one hand, examples were reported in which a Rh–Rh interaction was found for a metal–metal distance of 3 Å [15] but, on the other hand, Rh–Rh single bonds were shown to be only within the 2.6–2.8 Å range [16]. In our case, the Rh(1)–Rh(2) distance of 2.848(2) Å and the acute angles around the bridging atoms Rh(1)–C(1)–Rh(2) 89.6(7)°, Rh(1)–S(1)–Rh(2) 71.6(1)° and Rh(1)–S(2)–Rh(2) 73.7(1)° could lead to ambiguity. Therefore, we tackled this problem by performing EHMO theoretical calculations, which clearly show no overlap population for the Rh–Rh interaction in complex 7 (*vide infra*).

The distances Rh(1)–C(1) and Rh(2)–C(1) were found to be unequal (2.07(2) and 1.97(2) Å, respectively) primarily owing to the fact that the formal

TABLE 7. Selected bond lengths (Å) and angles (°) for 8 with e.s.d.s in parentheses

Bond lengths

Rh(1)–Rh(2)	2.873(1)	Rh(1)–C(1)	2.018(8)
Rh(1)–Cl(1)	2.502(2)	Rh(2)–Cl(1)	2.501(2)
Rh(1)–Cl(2)	2.455(2)	Rh(2)–Cl(3)	2.350(2)
Rh(1)–S	2.437(2)	Rh(2)–S	2.322(2)
Rh(1)–P(1)	2.263(2)	Rh(2)–P(3)	2.224(3)
Rh(1)–P(2)	2.322(2)	Rh(2)–C(1)	1.98(1)

Bond angles

Rh(2)–Rh(1)–Cl(1)	54.94(5)	Rh(1)–Rh(2)–Cl(1)	54.97(5)
Rh(2)–Rh(1)–Cl(2)	129.36(6)	Rh(1)–Rh(2)–Cl(3)	125.98(6)
Rh(2)–Rh(1)–S	51.04(6)	Rh(1)–Rh(2)–S	54.72(5)
Rh(2)–Rh(1)–P(1)	126.78(6)	Rh(1)–Rh(2)–P(3)	127.44(7)
Rh(2)–Rh(1)–P(2)	115.22(7)	Rh(1)–Rh(2)–C(1)	44.6(3)
Rh(2)–Rh(1)–C(1)	43.5(2)	Cl(1)–Rh(2)–Cl(3)	89.27(9)
Cl(1)–Rh(1)–Cl(2)	89.13(8)	Cl(1)–Rh(2)–S	85.41(8)
Cl(1)–Rh(1)–S	83.01(7)	Cl(1)–Rh(2)–P(3)	176.27(9)
Cl(1)–Rh(1)–P(1)	171.2(1)	Cl(1)–Rh(2)–C(1)	87.7(3)
Cl(1)–Rh(1)–P(2)	87.78(8)	Cl(3)–Rh(2)–S	172.03(9)
Cl(1)–Rh(1)–C(1)	86.9(2)	Cl(3)–Rh(2)–P(3)	90.9(1)
Cl(2)–Rh(1)–S	95.08(9)	Cl(3)–Rh(2)–C(1)	104.0(3)
Cl(2)–Rh(1)–P(1)	83.87(9)	S–Rh(2)–P(3)	94.04(9)
Cl(2)–Rh(1)–P(2)	94.95(9)	S–Rh(2)–C(1)	81.8(3)
Cl(2)–Rh(1)–C(1)	172.5(3)	P(3)–Rh(2)–C(1)	95.8(3)
S–Rh(1)–P(1)	92.24(8)	Rh(1)–Cl(1)–Rh(2)	70.10(6)
S–Rh(1)–P(2)	166.26(9)	Rh(1)–S–Rh(2)	74.23(8)
S–Rh(1)–C(1)	78.2(3)	Rh(1)–C(1)–Rh(2)	91.9(4)
P(1)–Rh(1)–P(2)	98.14(8)	Rh(1)–C(1)–O	138.9(6)
P(1)–Rh(1)–C(1)	99.4(2)	Rh(2)–C(1)–O	129.2(7)
P(2)–Rh(1)–C(1)	91.21(3)		

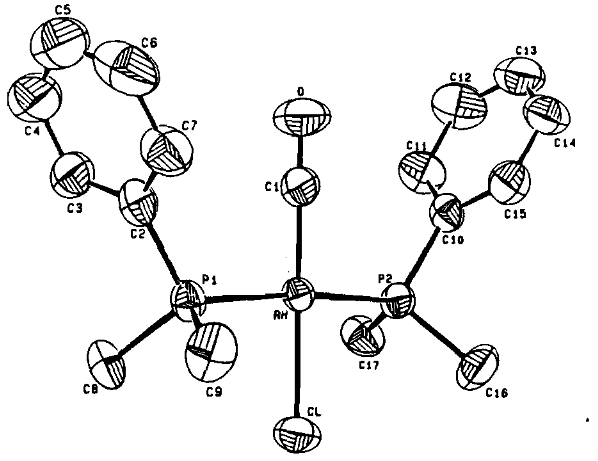

Fig. 1. ORTEP drawing of *trans*-RhCl(CO)[$(CH_3)_2PC_6H_5$]$_2$ (6) with the numbering scheme. Thermal ellipsoids scaled at 50% probability level. Hydrogen atoms are omitted for clarity.

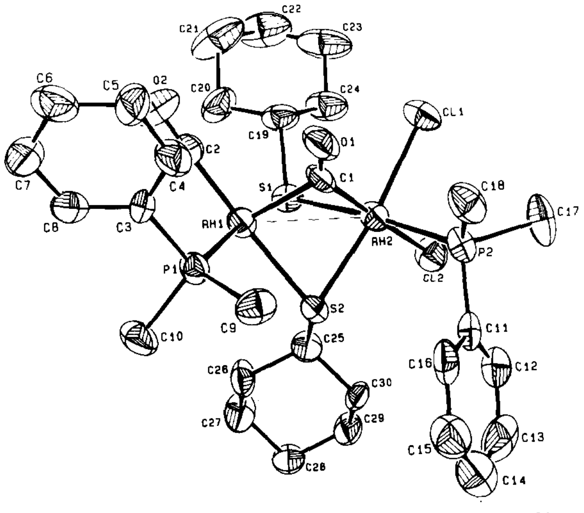

Fig. 2. ORTEP drawing of [$(CH_3)_2PC_6H_5$](CO)Rh(μ-CO)(μ-SC_6H_{11})$_2$RhCl$_2$[$(CH_3)_2PC_6H_5$] (7) with the numbering scheme. Thermal ellipsoids at 50% probability level. Hydrogen atoms are omitted for clarity.

valency numbers of Rh(1) and Rh(2) are different. Consequently the π-backdonation from the metal atoms to the carbonyl carbon is different as well [17]. Atom S(2) is closer to Rh(2) than to Rh(1) (bond lengths 2.358(4) and 2.390(4) Å, respectively) while S(1) is closer to Rh(1) than to Rh(2) (bond lengths 2.380(4) and 2.494(5) Å, respectively). This

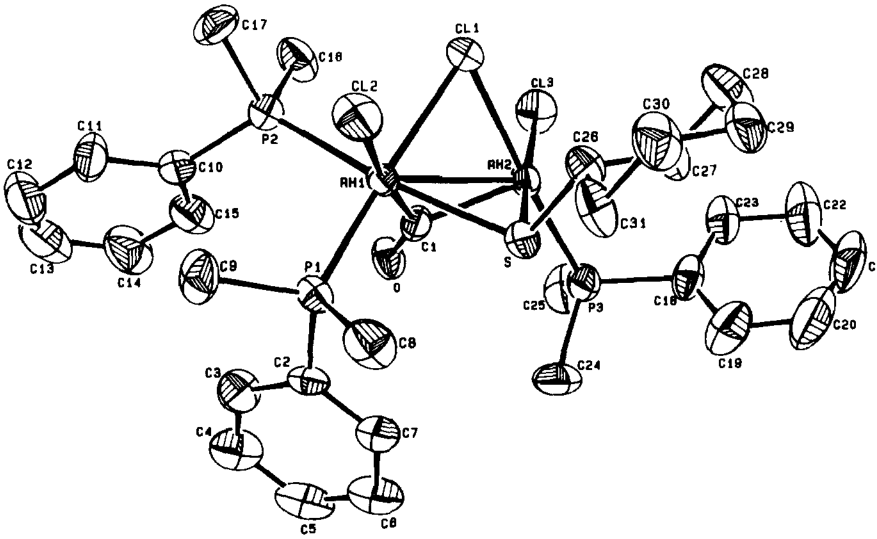

Fig. 3. ORTEP drawing of $[(CH_3)_2PC_6H_5]_2ClRh(\mu\text{-}CO)(\mu\text{-}Cl)(\mu\text{-}SC_6H_{11})RhCl[(CH_3)_2PC_6H_5]$ (8) with the numbering scheme. Thermal ellipsoids at 50% probability level. Hydrogen atoms are omitted for clarity.

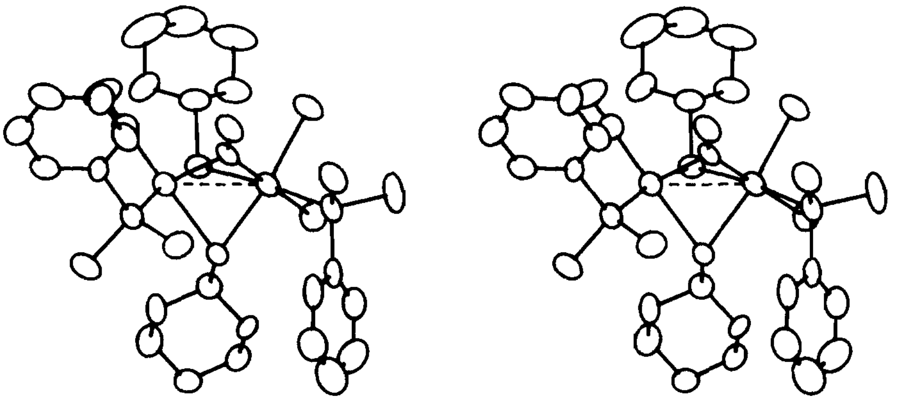

Fig. 4. Stereoscopic view of $[(CH_3)_2PC_6H_5](CO)Rh(\mu\text{-}CO)(\mu\text{-}SC_6H_{11})_2RhCl_2[(CH_3)_2PC_6H_5]$ (7).

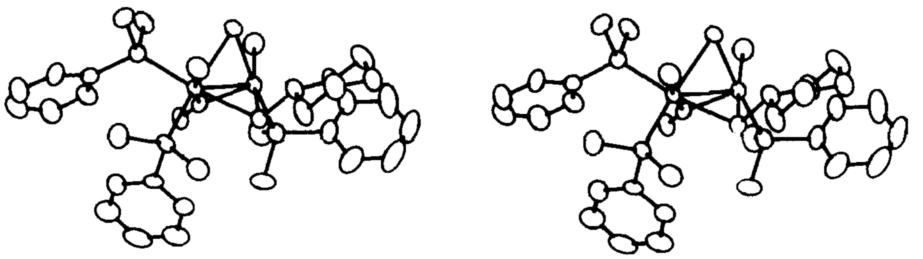

Fig. 5. Stereoscopic view of $[(CH_3)_2PC_6H_5]_2ClRh(\mu\text{-}CO)(\mu\text{-}Cl)(\mu\text{-}SC_6H_{11})RhCl[(CH_3)_2PC_6H_5]$ (8).

indicates that S(1) serves as electron donor to Rh(1) and S(2) to Rh(2).

The distance between Rh(1) and the terminal carbonyl carbon C(2) is considerably longer (1.90(2) Å) than the reported typical values for the Rh—C≡O bond of 1.76–1.83 Å in dirhodium carbonyls, in which the C≡O groups are *trans* to a bridging chlorine atom (see, for example, refs. 1 and 2). This observation reflects on the substantial *trans* effect transmitted by the bridging S(2) atom. The C(2)—O(2) distance 1.09(2) Å and the Rh(1)—C(2)—O(2) angle 177(2)° are as expected (see, for example, ref. 17).

The difference between the bond lengths of Rh(2)—Cl(1) and Rh(2)—Cl(2) (2.381(4) and 2.431(4) Å, respectively) reflects on the difference between the *trans* effect of the thiolato S(2) and that of the bridging carbonyl on the respective chlorine atoms.

In accord with the electronic nature of the two Rh atoms we found that 7 has no ESR spectrum. The ^{31}P NMR spectrum (in C_6D_6) which consists of two doublets at 0.638 (JPRh) = 124 Hz) and 10.952 ppm (J(PRh) = 118 Hz), reflexes on the differences between P(1) and P(2).

Like in 7, the two rhodium nuclei in 8 also have different coordination spheres (Fig. 3). Rh(1) forms a distorted octahedron and Rh(2) a square pyramid with the bridging carbonyl at the apical position. The metal atoms also share one Cl and one S atom. The Rh(1)–Rh(2) distance is 2.873(1) Å, i.e. somewhat longer than in 7, and the angles around the three bridging atoms are Rh(1)–Cl(1)–Rh(2) 70.10(6)°, Rh(1)–S–Rh(2) 74.23(8)° and Rh(1)–C(1)–Rh(2) 91.9(4)°, which again could lead to ambiguity. However, EHMO calculations (*vide infra*) indicate nearly equal charge distribution on Rh(1) and Rh(2), and some single bond character between them.

As in the former complex the bridging carbonyl in 8 is not centered exactly between the two metal atoms, although the difference between Rh(1)–C(1) (2.018(8) Å) and Rh(2)–C(1) (1.980(10) Å) is smaller than in 7. The elongation of the Rh(1)–C(1) bond is caused by the *trans* effect transmitted by Cl(2). The angles associated with these bonds, i.e. Rh(1)–C(1)–O and Rh(2)–C(1)–O are 138.9(6)° and 129.2(7)°, respectively. Thus, the correlation between the bond lengths and the angles in 8 is opposite to that expected, in general, for carbonyl bridged complexes [18].

Extended Hückel molecular orbital calculations [19] were performed using Hoffmann's program ICON 8 with weighted H_{ij} option (Program No. 469 obtained from the Quantum Chemistry Program Exchange), for the dirhodium complexes 7 and 8 in order to obtain the electron distribution and a qualitative molecular orbital picture of the bindings in these molecules. Similar calculations were carried out also for the mono-rhodium complex **6**, see 'Supplementary Material'. In all our calculations we used the actual geometric data obtained from the X-ray diffraction analyses. The atomic parameters employed are those listed in Table 8 [20].

Of the occupied MOs, the highest to which the metal still contributes in 7 ('MHOMO', not the actual HOMO) incorporates mainly d(yz) of Rh(2), and p(y) and p(z) of S(2). The metal-LUMO ('MLUMO', which does not coincide with the actual LUMO) incorporates mainly d(xz) of Rh(1), d(yz) of Rh(2) and p(z) of S(1). The energy gap E(MLUMO) – E(MHOMO) is –11.503 – (12.220) = 0.72 eV.

The Mulliken overlap population analysis and the reduced energy matrix (Table 9) led to interesting conclusions. While a positive overlap population corresponds to a net bonding between the atoms, a negative value represents an antibonding interaction [21]. The reduced energy matrix shows a particular contribution of the bonds to the total energy of the molecule; while a negative value reveals stabilization

TABLE 8. Extended Hückel parameters

Orbital		H_{ii} (eV)	Exponents ζ_1
H	1s	–13.6	1.3
C	2s	–21.4	1.625
C	2p	–11.4	1.625
O	2s	–32.3	2.275
O	2p	–14.8	2.275
P	3s	–18.6	1.60
P	3p	–14.0	1.60
Cl	3s	–30.0	2.033
Cl	3p	–15.0	2.033
Rh	5s	–8.09	2.135
Rh	5p	–4.57	2.10
Rh [a]	4d	–12.5	4.29 (0.5807) 1.97 (0.5685)

[a] ζ_1 and ζ_2 with the corresponding expansion coefficients.

TABLE 9. Overlap population and reduced energy matrices for selected atom pairs in 7

	Overlap population					Reduced energy (eV)			
	C(1)	C(2)	Rh(1)	Rh(2)		C(1)	C(2)	Rh(1)	Rh(2)
O(1)	1.12		–0.05	–0.05	O(1)	–36.60		1.47	1.20
O(2)		1.34	–0.05		O(2)		–42.90	1.36	
P(1)			–0.69		P(1)			–14.42	
P(2)				0.66	P(2)				–14.12
S(1)	0.02		0.65	0.50	S(1)	–0.41		–13.82	–10.61
S(2)	0.03		0.54	0.64	S(2)	–0.56		–11.30	–13.54
Cl(1)				0.40	Cl(1)				–10.30
Cl(2)				0.36	Cl(2)				–9.25
Rh(1)	0.41	0.75		0.002	Rh(1)	–9.46	–17.3	–78.00	
Rh(2)	0.54		0.002		Rh(2)	–12.52		–0.13	–71.90

(bonding), a positive figure corresponds to destabilization (antibonding).

The excess energy of Rh(2) indicates that the two metal atoms differ in stability and the pentacoordinated Rh(1) is the more stable one.

Both matrices show clearly that hardly any metal–metal interaction exists in complex 7. Thus, in spite of the relatively short Rh–Rh distance (*vide supra*) these atoms do not form a single bond linkage. The metal nuclei are connected with each other only through the three bridging groups, and in particular through the two sulfur atoms. These orbital interactions are shown in Fig. 6.

As expected the calculated net atomic populations listed in Table 10 indicate a higher positive charge on Rh(2) than on Rh(1). However, part of the excessive charge on the trivalent metal is distributed through the triple bridge.

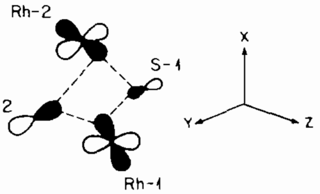

Fig. 6. Schematic interaction diagram of the two μ-SR bridges in 7.

TABLE 10. Net atomic population of selected atoms in compounds 7 and 8

Compound 7				Compound 8			
C(1)	0.81	S(1)	−0.21	C(1)	0.80	Cl(1)	−0.68
C(2)	0.78	S(2)	−0.30	O	−0.92	Cl(2)	−0.80
O(1)	−0.87	Cl(1)	−0.86	P(1)	−0.43	Cl(3)	−0.78
O(2)	−0.57	Cl(2)	−0.83	P(2)	−0.43	Rh(1)	1.86
P(1)	−0.45	Rh(1)	1.40	P(3)	−0.57	Rh(2)	1.72
P(2)	−0.43	Rh(2)	1.85	S	−0.12		

For 8 the energy gap between the MHOMO and the MLUMO at the metal was found to be $E(\text{MLUMO}) - E(\text{MHOMO}) = -11.589 - (-11.966) = 0.38$ eV (8.69 Kcal mol^{-1}).

The MHOMO incorporates mainly d(xy) and d(yz) of Rh(1) and d(z^2) of Rh(2). The MLUMO is composed mainly of −d(z^2) of Rh(1) and d(xz) of Rh(2).

The overlap population and reduced energy matrices given in Table 11 show that in contrast to 7 there is some interaction between the two rhodium atoms. This observation is rather surprising since the Rh(1)–Rh(2) distance in 8 is longer than in 7 (in which no Rh–Rh interaction was found) by 0.035 Å.

The Rh(1)–Rh(2) interaction that involves the d(xy) and d(z^2) orbitals of both atoms is depicted in Fig. 7.

As for 7 the two metal atoms differ in stability although to a smaller extent. Here too, the pentacoordinated atom is more stable than the hexacoordinated one.

The calculated net atomic populations (see Table 10) show that for 8 there is only a slight difference between the positive charges on Rh(1) and Rh(2). The distribution of the excessive charge may either take place through the single bond formed between the metal atoms (Fig. 7) or may involve the orbitals of the triple bridge shown in Fig. 8. Thus, in this complex the two rhodium atoms are formally divalent, and its paramagnetic nature could be shown

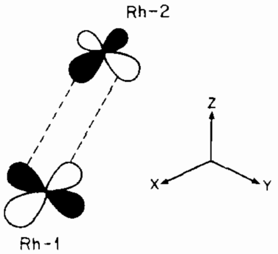

Fig. 7. Schematic Rh(1)–Rh(2) interaction in complex 8.

TABLE 11. Overlap population and reduced energy matrices for selected atom pairs in 8

	Overlap population				Reduced energy (eV)		
	C(1)	Rh(1)	Rh(2)		C(1)	Rh(1)	Rh(2)
O	1.07	−0.04	−0.06	O	−35.06	1.11	1.62
P(1)	0.02	0.07		P(1)	−0.50	−15.61	
P(2)	0.04	0.67		P(2)	−1.00	−14.2	
P(3)	0.03		0.79	P(3)	−0.67		−16.83
S	0.04	0.50	0.68	S	−0.99	−10.71	−14.80
Cl(1)		0.28	0.32	Cl(1)		−7.1	−7.8
Cl(2)		0.33		Cl(2)		−8.3	
Cl(3)			0.45	Cl(3)			−11.67
Rh(1)	0.47		0.08	Rh(1)	−10.01	72.2	
Rh(2)	0.49	0.08		Rh(2)	−11.58	−0.24	−75.08

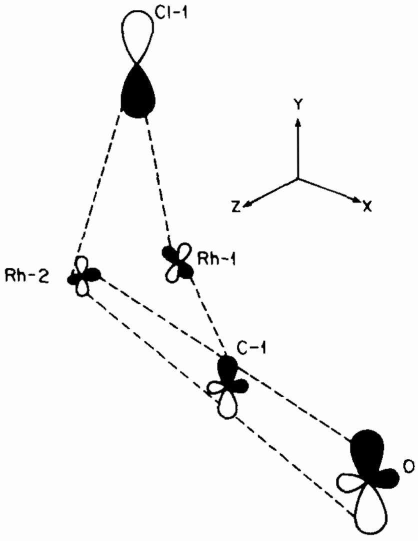

Fig. 8. Schematic interaction diagram of the μ-Cl and μ-CO bridges in 8.

by the low temperature (230 K) ESR spectrum $g_1 = 1.927$, $g_2 = 2.069$. At 300 K the ESR signals broaden owing to enhanced electron transfer between the two metal atoms.

In conclusion, the formation of the two unsymmetrical dirhodium complexes **7** and **8** can be rationalized by a rarely observed disproportionation of **1** by Me_2PhP (**4**) into the Rh(II) and Rh(0) species **11** and **12**, respectively (cf. ref. 17). Combination of two molecules of **11** may furnish either **13** or **14**. When the former compounds react with $Me_3SiSC_6H_{11}$ (**5**), **7** is formed. Interaction of **14** with **5** may yield **15**, which upon treatment with **5** yields **8** (see Scheme 1).

The formation of the 'normal' *cis*-$(Me_2PhP)(CO)Rh(\mu\text{-}Cl)(\mu\text{-}SC_6H_{11})Rh(CO)(Me_2PhP)$ (**9**) [1, 2, 12], its *trans*-isomer **10**, as well as the monorhodium complex **6**, is explained by an initial reaction of **1** with two molecules of **4**, followed by loss of CO that leads to compound **16**. (Application of an excess of the phosphine gives **6**.) Since the two metal atoms in

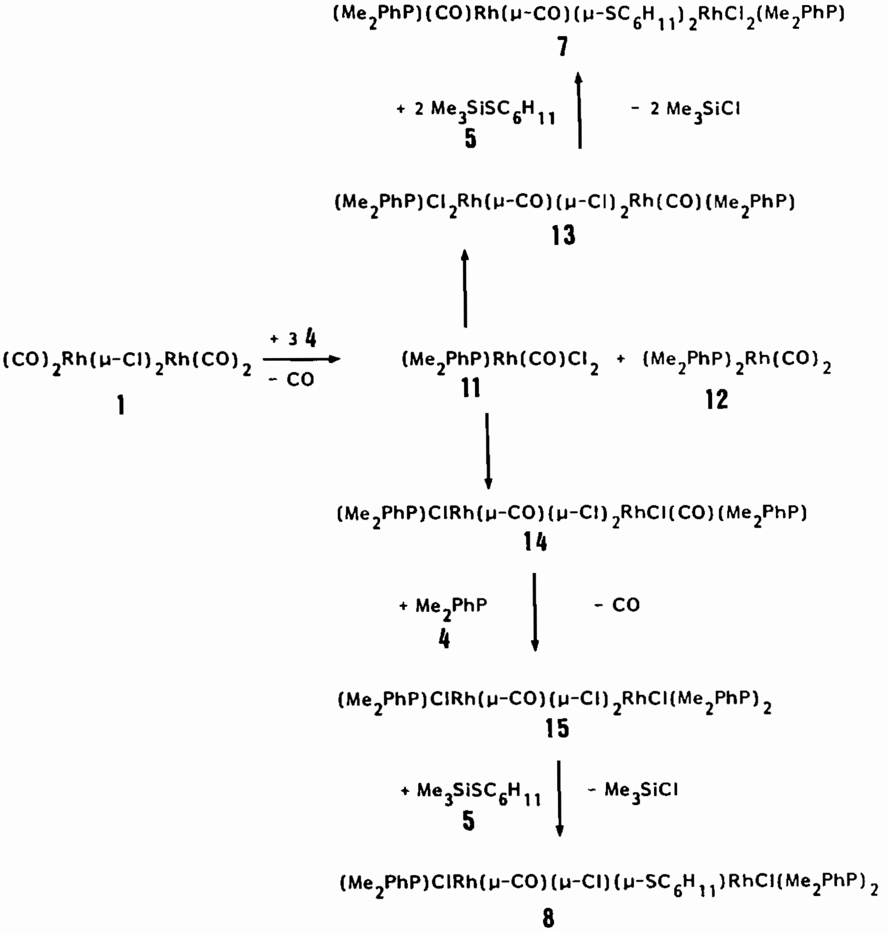

Scheme 1.

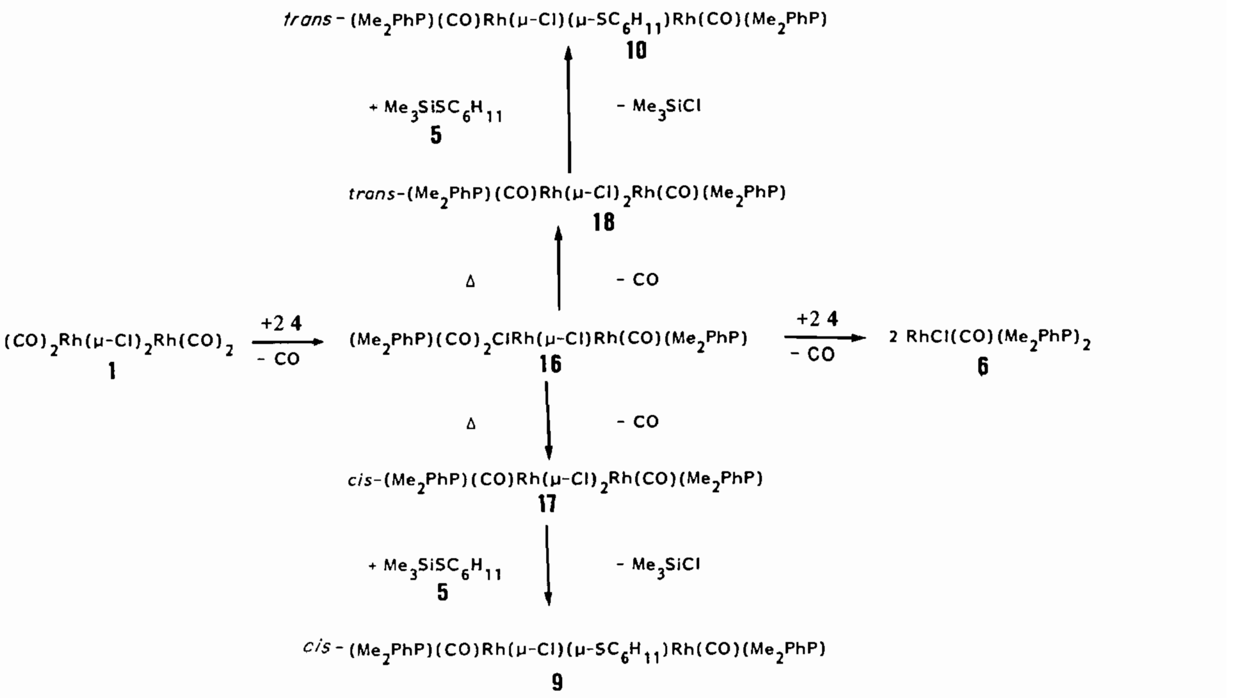

Scheme 2.

16 are bridged just by one chlorine, it may be transformed, upon decarbonylation, to both *cis*- and *trans*-$(Me_2PhP)(CO)Rh(\mu\text{-}Cl)_2Rh(CO)(Me_2PhP)$ (**17** and **18**, respectively, which, in turn, are converted by **5** into **9** and **10** (Scheme 2).

Although the sequence of some of the steps outlined in the Schemes may be exchanged, the various processes are assumed to summarize the general routes to the different products obtained in our laboratories from $[Rh(CO)_2]_2(\mu\text{-}Cl)_2$ (**1**), tertiary phosphines (or arsines) and trimethylsilyl thioethers [1, 2, 5, 12].

Supplementary Material

Listing of the thermal parameters and the values of observed and calculated structure factors for **6**, **7** and **8** as well as extended Hückel molecular orbital calculations for **6** are available from the authors upon request.

Acknowledgements

We wish to thank Dr Shmuel Cohen for his help in the X-ray analyses, Professor A. Y. Meyer for his help in the EHMO calculations and for most useful suggestions, the Deutsche Forschungsgemeinschaft and the Fonds der Chemischen Industrie for financial support of this study as well as Degussa for a valuable gift of rhodium chloride.

References

1 H. Schumann, G. Cielusek and J. Pickardt, *Angew. Chem., 92* (1980) 60; *Angew. Chem., Int. Ed. Engl., 19* (1980) 70.
2 H. Schumann, G. Cielusek, S. Jurgis, E. Hahn, J. Pickardt, J. Blum, Y. Sasson and A. Zoran, *Chem. Ber., 117* (1984) 2825.
3 M. Eisen, J. Blum, H. Schumann and S. Jurgis, *J. Mol. Catal., 31* (1985) 317.
4 M. Eisen, T. Bernstein, J. Blum and H. Schumann, *J. Mol. Catal., 43* (1987) 199.
5 H. Schumann, S. Jurgis, E. Hahn, J. Pickardt, J. Blum and M. Eisen, *Chem. Ber., 118* (1985) 2738.
6 H. Schumann and G. Cielusek, unpublished results.
7 R. S. Glass, *J. Organomet. Chem., 61* (1973) 83.
8 J. Chatt and B. L. Shaw, *J. Chem. Soc. A*, (1966) 1437.
9 G. M. Sheldrick, *SHELX 86*, program for crystal structure determination, University of Göttingen, F.R.G., 1986.
10 G. M. Sheldrick, *SHELX 76*, program for crystal structure determination, University of Cambridge, U.K., 1976.
11 M. Eisen, J. Blum, H. Schumann and B. Gorella, *J. Mol. Catal., 56* (1989) 330.
12 A. J. Deeming and P. J. Sharratt, *J. Organomet. Chem., 99* (1975) 447.
13 (a) M. A. Jennings and A. Wojcicki, *Inorg. Chem., 6* (1967) 1854; (b) B. L. Shaw, B. E. Marin and C. Masters, *J. Chem. Soc. A*, (1971) 1104.
14 See R. P. Hughes, in G. Wilkinson, F. G. A. Stone and E. W. Abel (eds.), *Comprehensive Organometallic Chemistry, The Synthesis, Reactions and Structures of Organometallic Compounds*, Vol. 5, Pergamon, Oxford, 1982, Ch. 35.

15 C. Claver, P. Kalck, M. Ridmy, A. Thorez, L. A. Oro, M. T. Pinillos, M. C. Apreda, F. H. Cono and C. Foces-Foces, *J. Chem. Soc., Dalton Trans.*, (1988) 1525, and refs. therein.

16 B. R. James, D. Mahajan, B. J. Rettig and G. M. Williams, *Organometallics, 2* (1983) 1452, and refs. therein.

17 M. Cowie and S. K. Dwight, *Inorg. Chem., 19* (1980) 2508.

18 F. A. Cotton, *Prog. Inorg. Chem., Radiochem., 21* (1976) 1.

19 J. H. Ammeter, H. B. Burgi, J. C. Thibeault and R. Hoffmann, *J. Am. Chem. Soc., 100* (1978) 3686.

20 (a) R. H. Summerville and R. Hoffmann, *J. Am. Chem. Soc., 98* (1976) 7240; (b) P. Kubacek, R. Hoffmann and Z. Halves, *Organometallics, 1* (1982) 180; (c) D. M. Hoffman and R. Hoffmann, *J. Am. Chem. Soc., 104* (1982) 4858.

21 M. D. Curtis, K.-B. Shiu and W. M. Butler, *J. Am. Chem. Soc., 108* (1986) 1550.